

Tetrameric Fluorophosphazene, (NPF<sub>2</sub>)<sub>4</sub>, Planar or Puckered?Anil J. Elias,<sup>†</sup> Brendan Twamley,<sup>†</sup> Ralph Haist,<sup>‡</sup> Heinz Oberhammer,<sup>‡</sup> Gerald Henkel,<sup>§</sup> Bernt Krebs,<sup>¶</sup> Enno Lork,<sup>#</sup> Ruediger Mews,<sup>#</sup> and Jean'ne M. Shreeve<sup>\*,†</sup>

Contribution from the Department of Chemistry, University of Idaho, Moscow, Idaho, 83844-2343, Institute for Physical and Theoretical Chemistry, University of Tuebingen, D-72076, Tuebingen, Germany, Gerhard-Mercator-University GHS Duisburg, Institute for Synthesechemie, Lotharstrasse 1, D-47057, Duisburg, Germany, Inorganic Chemistry Institute, University of Muenster, Wilhelm-Klemm-Strasse 8, D-48149, Muenster, Germany, and Institute of Inorganic and Physical Chemistry, University of Bremen, D-28334, Bremen, Germany

Received April 13, 2001

**Abstract:** The results obtained in a comprehensive experimental study on the redetermination of the structure of N<sub>4</sub>P<sub>4</sub>F<sub>8</sub> with single-crystal X-ray diffraction, gas electron diffraction (GED), and differential scanning calorimetry (DSC) establish clearly that, in contrast to the previous report, the eight-membered heterocycle is *not* planar. Above the phase transition temperature of  $-74$  °C, the ring appears pseudoplanar. However, the N<sub>4</sub>P<sub>4</sub> ring is disordered and is puckered above the phase transition when the disorder is modeled correctly. Below the phase transition the ring clearly resembles that of the saddle (K form) of N<sub>4</sub>P<sub>4</sub>Cl<sub>8</sub>. The unit cell of the low-temperature phase is derived from that of the higher temperature phase by doubling the *c*-axis and removing one-half of the symmetry elements. Full structure optimizations were performed at the HF/6-31G\* and B3LYP/6-31G\* levels and fully support the experimental diffraction data.

## Introduction

The currently accepted perfectly planar structure of tetrameric octafluorophosphazene, N<sub>4</sub>P<sub>4</sub>F<sub>8</sub>, whose crystal structure was determined at room temperature in 1961, stands out from the rest of the eight-membered inorganic heterocycles.<sup>1,2</sup> Paddock, in his review on phosphonitrilic compounds, has attributed the planarity of this phosphazene ring to the strong inductive influence of the fluorine atoms that permits the extensive delocalization of the lone pairs of the nitrogen atoms, with the consequent increase of the PNP bond angles.<sup>3</sup> It is also of interest to note that while the six-membered heterocycles, N<sub>3</sub>P<sub>3</sub>Cl<sub>6</sub> and N<sub>3</sub>P<sub>3</sub>F<sub>6</sub>, are planar, the perchloro tetramer, N<sub>4</sub>P<sub>4</sub>Cl<sub>8</sub>, is puckered and exists in two of the four potentially important nonplanar configurations of tetrameric rings.<sup>4</sup> However, Allcock, in his classic text on phosphorus–nitrogen compounds,<sup>5</sup> highlighted the conformational differences when X-ray structural data were compared to vibrational data. Based on infrared and Raman spectral calculations, N<sub>4</sub>P<sub>4</sub>F<sub>8</sub> was assigned a nonplanar

structure with a symmetry of C<sub>2h</sub> or lower.<sup>6,7</sup> Several theoretical studies<sup>8</sup> and structure determinations<sup>9</sup> of substituted tetrameric fluorophosphazenes have made use of the planar description of the structure of N<sub>4</sub>P<sub>4</sub>F<sub>8</sub> for comparison with experimental results and for substantiating theoretical calculations.

Recently, we have determined structures of several N<sub>4</sub>P<sub>4</sub>F<sub>8</sub> derivatives and have observed that in all instances, the eight-membered heterocycle is nonplanar.<sup>10</sup> This encouraged a reinvestigation of the molecular structure of the parent molecule N<sub>4</sub>P<sub>4</sub>F<sub>8</sub>. The structure was redetermined by using X-ray diffraction, gas electron diffraction, and differential scanning calorimetry. Results from each of these measurements unequivocally support a nonplanar eight-membered ring for N<sub>4</sub>P<sub>4</sub>F<sub>8</sub> that is puckered and that undergoes a phase transition at ca.  $-74$  °C. Details of the various analytical studies and their conclusions are described below.

## Experimental Section

**N<sub>4</sub>P<sub>4</sub>F<sub>8</sub> (1).** This compound was synthesized according to literature procedures<sup>11</sup> and purified by vacuum sublimation. Crystals of X-ray

<sup>†</sup> University of Idaho.<sup>‡</sup> University of Tuebingen.<sup>§</sup> Institute for Synthesechemie.<sup>¶</sup> University of Muenster.<sup>#</sup> University of Bremen.

(1) (a) Huheey, J. E.; Keiter, E. A.; Keiter, R. L. *Inorganic Chemistry: Principles of Structure and Reactivity*, 4th ed.; Harper Collins: New York, 1993; p 772. (b) Cotton, F. A.; Wilkinson, G.; Murillo, C. A.; Bochmann, M. *Advanced Inorganic Chemistry*, 6th ed.; John Wiley & Sons: New York, 1999; p 405. (c) Greenwood, N. N.; Earnshaw, E. A. *Chemistry of the Elements*, 2nd ed.; Butterworth & Heinemann: Boston, MA, 1998; p 537.

(2) (a) McGeachin, H. M.; Tromans, F. R. *J. Chem. Soc.* **1961**, 4777–4783. (b) McGeachin, H. M. *Chem. Ind.* **1960**, 1131. (c) Langer, J.; Seel, von F. Z. *Anorg. Alleg. Chem.* **1958**, 295, 316–326. (d) Jadodzinski, V. H.; Langer, J.; Oppermann, I.; Seel, von F. Z. *Anorg. Alleg. Chem.* **1959**, 302, 81–87. (e) Jadodzinski, V. H.; Oppermann, I. *Z. Krist.* **1960**, 113, 241–250.

(3) Paddock, N. L. *Quart. Rev.* **1964**, 18, 168.(4) Craig, D. P.; Paddock, N. L. *J. Chem. Soc.* **1962**, 4118–4133.(5) Allcock, H. R., *Phosphorus–nitrogen compounds; cyclic, linear, and high polymeric systems*; Academic Press: New York, 1972; p 49.(6) Becher, H. J.; Seel, F. Z. *Anorg. Alleg. Chem.* **1960**, 305, 148–157.(7) Chapman, A. C.; Paddock, N. L. *J. Chem. Soc.* **1962**, 635–644.

(8) (a) Breza, M. *Polyhedron* **2000**, 19, 389–397. (b) Mitchell, K. A. *R. J. Chem. Soc. (A)* **1968**, 2683–2688. (c) Faucher, J. P.; Labarre, J. F. *Phosphorus* **1974**, 3, 265–268. (d) Faucher, J. P.; Devanneaux, J.; Leibovici, C.; Labarre, J. F. *J. Mol. Struct.* **1971**, 10, 439–448. (e) Hoher, G.; Cstas, M.; Martin Polo, F. *Rev. Latinoam. Quim.* **1977**, 8, 110. (f) Ferris, K. F.; Duke, C. B. *Int. J. Quantum Chem., Quantum Chem. Symp.* **1989**, 23, 397. (g) Ranganathan, T. N.; Todd, S. M.; Paddock, N. L. *Inorg. Chem.*, **1973**, 12, 316–323.

(9) (a) Begley, M. J.; Millington, D.; King, T. J.; Sowerby, D. B. *J. Chem. Soc., Dalton Trans.* **1974**, 1162–1165. (b) Marsh, W. C.; Trotter, J. *J. Chem. Soc. (A)* **1971**, 569–572. (c) Marsh, W. C.; Trotter, J. *J. Chem. Soc. (A)* **1971**, 573–576. (d) Millington, D.; King, T. J.; Sowerby, D. B. *J. Chem. Soc., Dalton Trans.* **1973**, 396–399.

(10) (a) Elias, A. J.; Twamley, B.; Shreeve, J. M. *Inorg. Chem.* **2001**, 40, 2120–2126. (b) Lork, E.; Boehler, D.; Mews, R. *Angew. Chem., Int. Ed. Engl.* **1995**, 34, 2696.

**Table 1.** Crystal Data and Structure Refinement for **1a/1b**, **1c**, and **1d**

	<b>1a/1b</b>	<b>1c<sup>a</sup></b>	<b>1d</b>
empirical formula	N <sub>4</sub> P <sub>4</sub> F <sub>8</sub>	N <sub>4</sub> P <sub>4</sub> F <sub>8</sub>	N <sub>4</sub> P <sub>4</sub> F <sub>8</sub>
FW	331.92	331.96	331.92
cryst syst; space group <sup>b</sup>	monoclinic, <i>P2(1)/a</i>	monoclinic, <i>P2(1)/a</i>	monoclinic, <i>P2(1)/a</i>
color, habit	colorless block	colorless sphere	colorless block
cryst dimens, mm	0.50 × 0.38 × 0.18	0.8 × 0.8 × 0.8	0.50 × 0.50 × 0.25
<i>T</i> (°C)	232(2)	room temperature	172(2)
<i>a</i> (Å)	7.3580(11)	7.40	7.3848(7)
<i>b</i> (Å)	13.784(2)	13.83	13.8261(13)
<i>c</i> (Å)	4.9786(7)	5.16	9.6630(9)
$\beta$ (deg)	109.161(2)	109.5	109.461(2)
<i>V</i> (Å <sup>3</sup> )	476.96(12)	500	930.25(15)
<i>Z</i>	2	2	4
<i>D</i> <sub>calc</sub> (Mg m <sup>-3</sup> )	2.311	2.20	2.370
$\mu$ (mm <sup>-1</sup> )	0.893	0.88	0.916
$\lambda$ (Å)	0.71073	0.71073	0.71073
final <i>R</i> indices [ <i>I</i> > 2 $\sigma$ ( <i>I</i> )] <sup>c</sup>	<i>R</i> <sub>1</sub> = 0.0341/0.0325 <i>wR</i> <sub>2</sub> = 0.0879/0.0849	<i>R</i> <sub>1</sub> = 0.102	<i>R</i> <sub>1</sub> = 0.0258 <i>wR</i> <sub>2</sub> = 0.0733
<i>R</i> indices (all data)	<i>R</i> <sub>1</sub> = 0.0372/0.0355 <i>wR</i> <sub>2</sub> = 0.0898/0.0868		<i>R</i> <sub>1</sub> = 0.0299 <i>wR</i> <sub>2</sub> = 0.0755

<sup>a</sup> Data from ref 2a. <sup>b</sup> Nonstandard setting of *P2(1)/c*. <sup>c</sup>  $R = \sum |F_o| - |F_c| / \sum |F_o|$ ;  $wR_2 = \{\sum [w(F_o^2 - F_c^2)^2] / \sum [w(F_o^2)^2]\}^{1/2}$ .

quality were grown by slow careful sublimation of the compound in a ~15 cm long tube by maintaining a differential temperature between the ends of the tube.

**X-ray Crystallographic Studies.** The crystals were removed from the vessel and immediately covered with a layer of hydrocarbon oil. A suitable crystal was selected, quickly attached to a glass fiber, and immediately placed in the low-temperature nitrogen stream.<sup>12</sup> Data were collected at 232(2) K (**1a,b**) and 172(2) K (**1d**) with use of a Siemens SMART 1K CCD instrument with Mo K $\alpha$  radiation ( $\lambda = 0.71073$  Å) and equipped with a LT-2A low-temperature device. The SHELXTL v. 5.10 program suite was used for structure solution and refinements.<sup>13</sup> Absorption corrections were applied by using the SADABS v. 6.02 program.<sup>14</sup> The crystal structures were solved by direct methods with the nonstandard setting of *P2(1)/a* used for all solutions in accordance with the original structure determination. They were refined by full-matrix least-squares procedures. All atoms were refined anisotropically except those involved in disorder in **1b**, which were held isotropic. The occupancy of the disorder in **1b** was refined as 54% for N1a and N2a and 46% for N1b and N2b. Some details of the data collection and refinement are given in Table 1. Further details are provided in the Supporting Information.

**Gas Electron Diffraction Studies.** The gas electron diffraction intensities were recorded with a Gasdiffraktograph KD-G2<sup>15</sup> at two nozzle-to-plate distances (25 and 50 cm) and with an accelerating voltage of ca. 60 kV. The sample reservoir was kept at 0 °C and the gas nozzle was at room temperature. The camera pressure during the experiments did not exceed 10<sup>-5</sup> Torr. The photographic plates (KODAK Electron Image, 13 × 18 cm) were analyzed with the usual methods<sup>16</sup> and averaged molecular intensities in the *s* ranges 2–18 and 8–35 Å<sup>-1</sup> ( $s = 4\pi/\lambda \sin \theta/2$ , where  $\lambda$  is the electron wavelength and  $\theta$  the scattering angle) in intervals of  $\Delta s = 0.2$  Å<sup>-1</sup>. Details are included in the Supporting Information.

## Results and Discussion

**Crystal Structures.** The original structure analysis of N<sub>4</sub>P<sub>4</sub>F<sub>8</sub> (**1c**) showed the inorganic eight-membered ring to be quasi-planar. However, McGeachin et al. clearly outline the physical problems associated with data collection for this compound.<sup>2</sup>

(11) Moeller, T.; Tsang, F. *Inorg. Synth.* **1967**, 9, 78–80.

(12) Hope, H. *Prog. Inorg. Chem.* **1995**, 41, 1–19.

(13) SHELXTL version 5.10; Structure Determination Software Suite; Bruker AXS Inc.: Madison, WI, 1998.

(14) SADABS, an absorption correction program for CCD SMART systems; Bruker AXS, Inc.: Madison WI, 1999.

(15) Oberhammer, H. *Molecular Structure by Diffraction Methods*; The Chemical Society: London, UK, 1976; Vol. 4, p 24.

(16) Oberhammer, H.; Gombler, W.; Willner, H. *J. Mol. Struct.* **1981**, 70, 273.

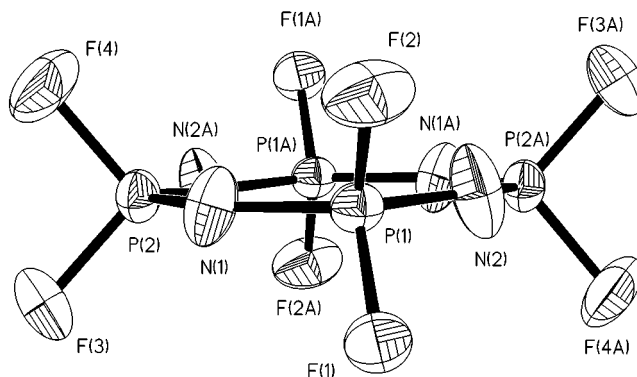


**Figure 1.** ORTEP diagram of **1a** at  $-41$  °C.

Data were collected at room temperature and high thermal motion was observed. **1c** has a low melting point and sample stability within a sealed Lindemann tube proved problematic. Although another crystalline form was observed at low temperature with a doubling of an axis, there are no reports of a low-temperature structure refinement. Despite the problems associated with the structure of **1c**, the quasiplanar model has been accepted to date in the literature. The P–N bond lengths show no appreciable alternation with an average of 1.507(17) Å. Bond angles of P–N–P = 147.2(1.4)° and N–P–N = 122.7(1.0)° were reported. Our study of this compound shows the existence of a phase transition. This was studied by a variety of methods: powder and single crystal diffraction and more precisely thermal differential scanning calorimetry (DSC). The phase transition temperature ranges from  $-72$  to  $-76$  °C, with the average at  $-74$  °C. This results in two clear modifications of the structure of **1**. At temperatures above this transition temperature (**1a** and **1b**), the cell parameters closely resemble those of **1c**. Below the transition temperature (**1d**) the cell parameters are similar except for the doubling of the *c*-axis.

**Modifications 1a, 1b, and 1c.** The modifications above the phase transition, **1a** and **1b**, have the same cell parameters as **1c**. Precise data were collected at  $-41$  °C to compare with the original solution of McGeachin et al. (**1c**).<sup>2</sup> The data were transformed into the nonstandard space group *P2(1)/a* to allow direct comparison with **1c**. The primary solution (**1a**, Figure 1) shows a planar ring system with P–N bond distances that are basically equal with an average P–N distance of 1.521(3) Å and P–N–P and N–P–N angles of 146.6(2)° and 123.2(2)°,

**Table 2.** Selected Bond Lengths and Bond Angles for **1a–d**<sup>a</sup>

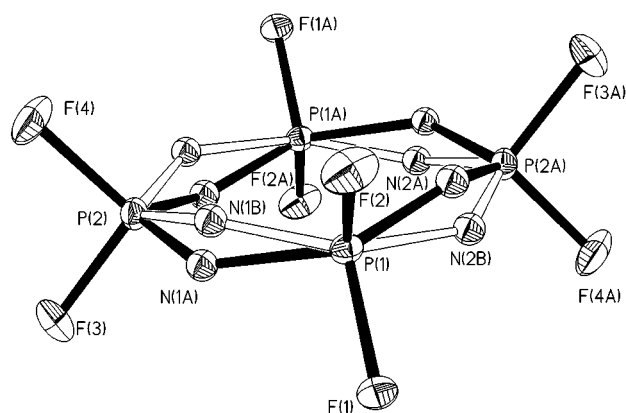
<b>1a</b>		<b>1b</b>		<b>1c<sup>b</sup></b>		<b>1d</b>	
(a) bond lengths (Å)							
P(1)–N(1)	1.526(3)	P(1)–N(1A)	1.591(6)	P(1)–N(2)	1.487(16)	P(1)–N(1)	1.546(2)
P(1)–N(2)	1.513(3)	P(1)–N(2A)	1.470(5)	P(1)–N(1)	1.523(16)	P(1)–N(4)	1.536(2)
P(2)–N(1)	1.528(3)	P(2)–N(1A)	1.530(5)	P(2)–N(2)	1.508(17)	P(2)–N(1)	1.544(2)
P(2)–N(2)#1	1.517(3)	P(2)–N(2A)#1	1.610(6)	P(2)–N(1)#1	1.510(17)	P(2)–N(2)	1.545(2)
P(1)–F(1)	1.508(2)	P(1)–N(1B)	1.490(7)	P(1)–F(3)	1.533(16)	P(3)–N(2)	1.549(2)
P(1)–F(2)	1.509(2)	P(1)–N(2B)	1.623(7)	P(1)–F(4)	1.500(13)	P(3)–N(3)	1.546(2)
P(2)–F(3)	1.520(2)	P(2)–N(1B)	1.557(7)	P(2)–F(1)	1.526(15)	P(4)–N(3)	1.540(2)
P(2)–F(4)	1.522(2)	P(2)–N(2B)#1	1.460(6)	P(2)–F(2)	1.499(16)	P(4)–N(4)	1.541(2)
		P(1)–F(1)	1.508(2)			P(1)–F(1)	1.522(1)
		P(1)–F(2)	1.518(2)			P(1)–F(2)	1.522(1)
		P(2)–F(3)	1.508(2)			P(2)–F(3)	1.528(1)
		P(2)–F(4)	1.508(2)			P(2)–F(4)	1.529(1)
						P(3)–F(5)	1.523(1)
						P(3)–F(6)	1.520(1)
						P(4)–F(7)	1.529(1)
						P(4)–F(8)	1.522(1)
(b) angles (deg)							
N(1)–P(1)–N(2)	123.28(17)	N(1A)–P(1)–N(2A)	125.5(3)	N(2)–P(1)–N(1)	122.3(1.04)	N(1)–P(1)–N(4)	123.37(8)
N(1)–P(2)–N(2)#1	123.18(17)	N(1A)–P(2)–N(2A)#1	121.3(3)	N(2)–P(2)–N(1)#1	123.2(0.96)	N(1)–P(2)–N(2)	122.97(9)
P(1)–N(1)–P(2)	143.7(2)	P(1)–N(1A)–P(2)	136.8(5)	P(1)–N(2)–P(2)	147.2(1.43)	N(2)–P(3)–N(3)	122.72(9)
P(1)–N(2)–P(2)#1	149.4(2)	P(1)–N(2A)–P(2)#1	143.1(5)	P(1)–N(1)–P(2)#1	147.1(1.36)	N(3)–P(4)–N(4)	123.27(9)
F(1)–P(1)–F(2)	98.10(13)	F(1)–P(1)–F(2)	98.10(13)	F(3)–P(1)–F(4)	99.5(0.86)	P(1)–N(1)–P(2)	139.70(11)
F(3)–P(2)–F(4)	98.64(16)	F(3)–P(2)–F(4)	98.58(16)	F(1)–P(2)–F(2)	100.3(0.90)	P(2)–N(2)–P(3)	139.23(11)
		N(1B)–P(1)–N(2B)	121.8(3)			P(3)–N(3)–P(4)	139.14(11)
		N(1B)–P(2)–N(2B)#1	119.3(4)			P(4)–N(4)–P(1)	143.52(11)
		P(1)–N(1B)–P(2)	144.4(5)			F(1)–P(1)–F(2)	99.24(8)
		P(1)–N(2B)–P(2)#1	142.8(6)			F(3)–P(2)–F(4)	99.07(6)
						F(5)–P(3)–F(6)	99.82(8)
						F(7)–P(4)–F(8)	98.89(7)

<sup>a</sup> Symmetry transformations used to generate equivalent atoms: #1  $-x, -y, -z$ . <sup>b</sup> Data from ref 2 arranged to match **1a**.

**Table 3.** Out-of-Plane Calculations (Å) for **1a–d** Based on the Best Plane through P Atoms

atom	<b>1a</b>	<b>1b</b>	<b>1c</b>	atom	<b>1d</b>
N(1)	-0.010	-0.205	0.243	N(1)	-0.211
P(1)	0	0	0	P(1)	0.011
N(2)	0.063	0.318	-0.251	N(2)	0.415
P(2)	0	0	0	P(2)	-0.011
N(1)#	0.010	0.205	-0.243	N(3)	-0.271
P(1)#	0	0	0	P(3)	0.011
N(2)#	-0.063	-0.318	0.251	N(4)	0.303
P(2)#	0	0	0	P(4)	-0.011

respectively (see Table 2). Plane calculations of N1–P1–N2–P2 show that deviations from true planarity are small and are almost identical to those observed in **1c** and are given in Table 3. However, the thermal parameters for the nitrogen atoms are elongated normal to the plane of the ring and are anomalously high. This led to the development of a disordered model with the nitrogen atom positions split into two positions. This affords the model represented as **1b** in Figure 2. Due to the disorder, the conformation is ambiguous and could be modeled as either chair or saddle. Therefore, the conformation cannot be assigned by using this technique. This ambiguity is also confirmed by GED analysis, which is discussed later. No constraints were imposed on the refinement and the occupancies and bond lengths of each disordered part were allowed to refine freely. In this model there are two superimposed  $N_4P_4F_8$  molecules related by inversion symmetry. The asymmetric unit consists of a half molecule of each disordered molecule and the disordered nitrogen atoms show refined N1a/N1b occupancies that are essentially equal, 54% and 46%, respectively. Bond lengths and angles in **1a** and **1c** are very similar. However, using this unconstrained model for **1b**, P–N bond alternation is observed in each disordered moiety, ranging from 1.623(7) to 1.460(6) Å.

**Figure 2.** ORTEP diagram of **1b**. Thermal displacement ellipsoids are shown at the 10% probability level. Only the symmetry unique nitrogen atoms are labeled.

This gives the appearance of a separation into  $\sigma$  and  $\sigma + \pi$  bond alternation. This is not seen in the closely related  $N_4P_4Cl_8$  species, which exists in two forms, boat and chair.<sup>17</sup> It has also been observed that ring bond lengths vary only when different groups are distributed unsymmetrically on the ring.<sup>18</sup> Therefore, this bond alternation is an artifact of the disordered model, a systematic deviation from the average P–N bond distances found in **1a**, (1.521(3) Å).

**Modification 1d.** The apparent center of symmetry present in the disordered high-temperature form (**1a** and **1b/1c**) dis-

(17) (a) Hazekamp, R.; Migchelsen, T.; Vos, A. *Acta Crystallogr.* **1962**, *15*, 539–543. (b) Wagner, A. J.; Vos, A. *Acta Crystallogr.* **1968**, *B24*, 707–713.

(18) (a) Allen, C. W.; Paul, I. C.; Moeller, T. *J. Am. Chem. Soc.* **1967**, *89*, 6362. (b) Mani, N. V.; Ahmed, F. R.; Barnes, W. H. *Acta Crystallogr.* **1965**, *19*, 693. (c) Mani, N. V.; Ahmed, F. R.; Barnes, W. H. *Acta Crystallogr.* **1965**, *21*, 375.



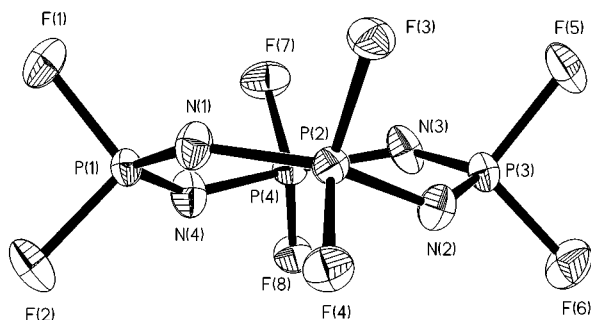


**Figure 3.** ORTEP diagram of **1d** at  $-101\text{ }^{\circ}\text{C}$ . Thermal displacement ellipsoids are shown at the 30% probability level.

appears in the ordered low-temperature form (**1d**). The cell is slightly different: the *c*-axis is doubled and only one-half of the symmetry elements are present. This results in the structure shown in Figure 3. No disorder is observed and a clear saddle conformation ( $S_4$ ) is seen. The phosphorus atoms practically lie in a plane with small out-of-plane (o.o.p) deviations and form a square. The nitrogen atoms alternate above and below this plane to a greater degree than seen in **1b**. In this case there is no P–N bond alternation and bond lengths comparable to **1a** and **1c** are seen. The average P–N bond distance is  $1.543(2)\text{ \AA}$ . P–N–P and N–P–N bond angles average  $140.4(1)^{\circ}$  and  $123.1(1)^{\circ}$ , respectively. The structure of **1d** bears a close resemblance to the saddle form of  $\text{N}_4\text{P}_4\text{Cl}_8$ , which has P–N bond lengths ranging from  $1.555(5)$  to  $1.562(6)\text{ \AA}$  and P–N–P and N–P–N angles of  $135.6(4)^{\circ}$  and  $120.6(3)^{\circ}$ , respectively.<sup>17b</sup> The differences in angles between **1d** and  $\text{N}_4\text{P}_4\text{Cl}_8$  are slight and can be accounted for by the higher electronegativity of the fluorine substituents. Using Bent's rule, the highly polarized P–F bonding would be higher in p-character, reducing the F–P–F angle ( $\text{Cl–P–Cl} = 103.1(1)^{\circ}$ ;  $\text{F–P–F} = 99.3(7)^{\circ}$ ), leaving more s-character on the phosphorus for bonding.<sup>19</sup> This results in wider angles and shorter bonding to the phosphorus atom as is seen experimentally. The packing diagram (Figure 4) shows that there are no significant intermolecular interactions with the closest distance being an  $\text{F}\cdots\text{F} = 2.985(3)\text{ \AA}$ .

**Gas-Phase Structure.** The gas-phase structure was determined by gas electron diffraction (GED). The radial distribution function (RDF) was derived by Fourier transform of the electron diffraction molecular intensities applying an artificial damping function  $\exp(-\gamma s^2)$  with  $\gamma = 0.0019\text{ \AA}^2$ . Analysis of the RDF shown in Figure 5 demonstrates that the ring deviates from planarity. For a planar structure ( $D_{4h}$  symmetry) nonbonded  $\text{P}\cdots\text{F}$  distances  $\text{P1}\cdots\text{F2}$  and  $\text{P1}\cdots\text{F2}'$  would be equal and this is not compatible with the peak between  $3.3$  and  $4.0\text{ \AA}$ . In the least-squares fit of the molecular intensities a diagonal weight function was applied to the intensities. Assuming all N–P–N and all P–N–P angles to be equal and furthermore assuming  $C_{2v}$  symmetry for the N–PF<sub>2</sub>–N moieties, five different symmetries for ring structures have to be considered: the planar  $D_{4h}$  symmetry and the nonplanar  $C_{4v}$ ,  $C_{2h}$ ,  $D_{2d}$ , and  $S_4$  symmetries.

In the  $C_{4v}$  model all phosphorus atoms and all nitrogen atoms lie in two parallel planes and the nonbonded distances  $\text{P1}\cdots\text{F2} \neq \text{P1}\cdots\text{F2}'$  and  $\text{P1}\cdots\text{F3} \neq \text{P1}\cdots\text{F3}'$ . (See atom numbering in Figure 5.) In a  $C_{2h}$  structure all ring atoms are in the plane, except two opposite phosphorus atoms which lie above and below this plane. If the ring possesses  $D_{2d}$  symmetry, all

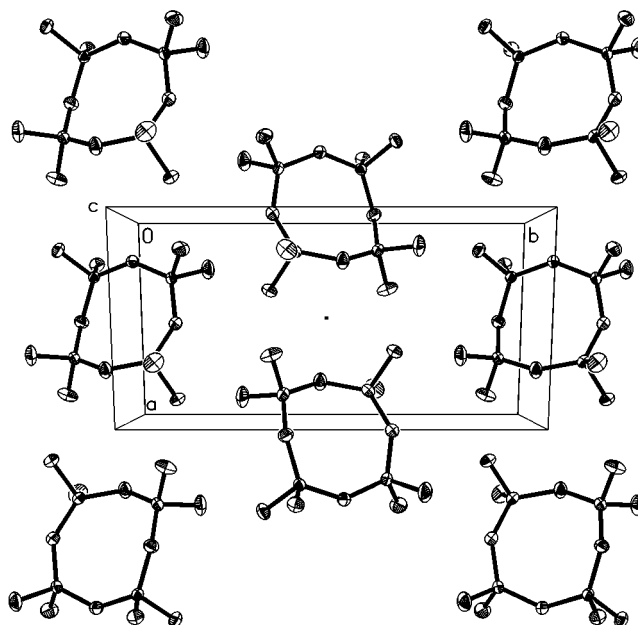


**Figure 4.** Packing diagram of **1d**. Thermal displacement ellipsoids are shown at the 30% probability level.

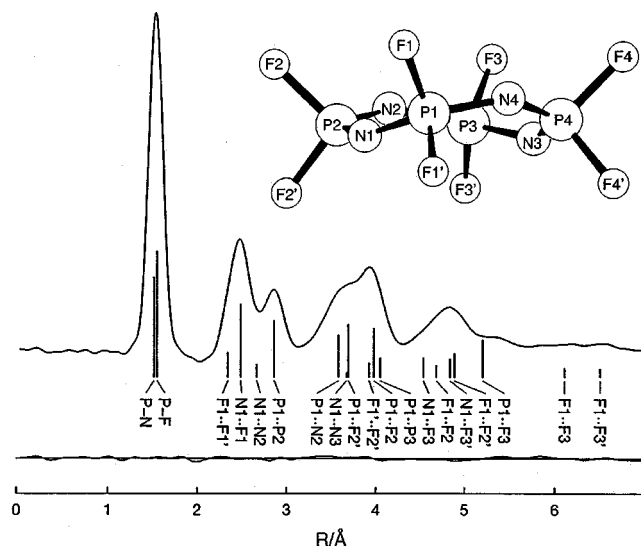


**Figure 5.** Experimental radial distribution function and difference curve. The positions of interatomic distances are indicated by vertical bars.

phosphorus atoms lie in a plane and two opposite nitrogen atoms (N1 and N3) above and the other two nitrogen atoms (N2 and N4) below this plane. In this case  $\text{P1}\cdots\text{F2} \neq \text{P1}\cdots\text{F2}'$  and  $\text{P1}\cdots\text{F3} = \text{P1}\cdots\text{F3}'$ . For  $S_4$  symmetry the signs of the out-of-plane coordinate (o.o.p) of the phosphorus and nitrogen atoms alternate (+, −, +, −) with different values for P and N.  $D_{2d}$  is a special case of  $S_4$  symmetry with zero o.o.p. coordinates for phosphorus.

Least-squares refinements were performed for a planar ring and for the four possible nonplanar symmetries. Since these models differ primarily by long nonbonded  $\text{P}\cdots\text{F}$  distances ( $R > 4\text{ \AA}$ ), the agreement factor for the long-camera-distance data ( $R_{50}$ ) is most sensitive toward the quality of the fit. For the planar conformation ( $D_{4h}$ )  $R_{50}$  is about three times larger than for all nonplanar structures. An equally good fit is obtained for  $S_4$  symmetry ( $R_{50} = 2.64\%$ ) and  $D_{2d}$  symmetry ( $R_{50} = 2.63\%$ ). The agreement factors for  $C_{4v}$  and  $C_{2h}$  models are 30 and 40% larger, respectively. For the  $S_4$  conformation, the refined o.o.p.

(19) (a) Bent, H. A. *Chem Rev.* **1961**, *61*, 275–311. (b) Shustorovich, E. *J. Am. Chem. Soc.* **1978**, *100*, 7513–7522. (c) Reed, A. E.; Schleyer, P. v. R. *J. Am. Chem. Soc.* **1987**, *109*, 7362–7373. (d) Gilheany, D. G. *Chem. Rev.* **1994**, *94*, 1339–1374 and references cited therein.

**Table 4.** Geometric Parameters of **1** from GED, X-ray Crystallography, and Ab Initio Calculations

	GED <sup>a</sup> S <sub>4</sub>		HF/6-31G*	B3LYP/6-31G*
	X-ray <sup>b</sup>	S <sub>4</sub>	S <sub>4</sub>	S <sub>4</sub>
P–N	1.520 (5)	1.543 (2)	1.542	1.568
P–F	1.554 (5)	1.524 (1)	1.536	1.566
P–N–P	141.2 (9)	140.4 (1)	146.6	139.6
N–P–N	122.9 (10)	123.2 (2)	120.9	122.2
F–P–F	98.0 (6)	99.3 (7)	99.3	99.4
Φ(P–N–P–N)	30.4 (22)	27.5	21.1	33.2
Φ(N–P–N–P)	26.6 (48)	28.7	19.0	32.5
o.o.p. (N) <sup>c</sup>	±0.299 (22)	±0.224	±0.187	±0.363
o.o.p. (P) <sup>c</sup>	±0.031 (63)	±0.011	±0.018	±0.006

<sup>a</sup> Gas-phase structure,  $r_a$  parameters with  $3\sigma$  uncertainties. <sup>b</sup> **1d** data (mean values) with  $\sigma$  uncertainties. <sup>c</sup> Out-of-plane coordinates of nitrogen and phosphorus atoms, respectively.

coordinates of the phosphorus atoms are  $\pm 0.031(63)$  Å, i.e., zero within the experimental uncertainty ( $3\sigma$  value). Thus,  $D_{2d}$  and  $S_4$  models are indistinguishable in the GED analysis. The bond lengths and bond angles obtained with these two symmetries are identical. Since quantum chemical calculations (see below) indicate that only the  $S_4$  conformer corresponds to a minimum on the energy hypersurface, the results for this structure are given in Table 4. Six geometric parameters (P–N, P–F, P–N–P, N–P–N, F–P–F, and the o.o.p. coordinate of P) and twelve vibrational amplitudes were refined simultaneously for the  $S_4$  conformer. Six correlation coefficients had values larger than  $|0.7|$ : PN/PF =  $-0.92$ , PN/PNP =  $-0.86$ , PN/NPN =  $-0.72$ , PF/PNP =  $0.78$ , PF/NPN =  $0.72$ , and PNP/NPN =  $0.88$ . Despite these large correlations, all geometric parameters are well determined by the six peaks of the RDF (see Figure 5), except for the o.o.p. coordinate of phosphorus.

### Theoretical Calculations

Full structure optimizations were performed at the HF/6-31G\* and B3LYP/6-31G\* level by using starting geometries of  $D_{4h}$  (planar ring),  $D_{2d}$ ,  $S_4$ ,  $C_{4v}$ , and  $C_{2h}$  symmetries. The starting geometries were defined by Cartesian coordinates. The optimized planar ring ( $D_{4h}$ ) possesses two imaginary frequencies, i.e., it does not correspond to a stable structure. Similarly, the  $D_{2d}$  form with o.o.p. coordinates for nitrogen of  $\pm 0.154$  (HF) and  $\pm 0.366$  Å (B3LYP) does not correspond to a minimum (one imaginary frequency). Starting geometries with  $C_{4v}$  or  $C_{2h}$  symmetry converge toward planar structures. Only the conformer with  $S_4$  symmetry corresponds to a stable structure. It possesses very small o.o.p. coordinates for phosphorus of  $\pm 0.018$  (HF) or  $\pm 0.006$  Å (B3LYP) and thus it is very similar to the  $D_{2d}$  form and it is not surprising that GED cannot distinguish between these two structures. The energy of the  $S_4$  conformer is  $0.24$  (HF) or  $0.61$  kcal mol<sup>-1</sup> (B3LYP) lower than that of the planar  $D_{4h}$  structure. The calculated five o.o.p. vibrations lie between  $17$  and  $52$  cm<sup>-1</sup> (B3LYP) and indicate a very flat energy hypersurface for o.o.p. motions. All quantum chemical calculations were performed with the GAUSSIAN98 program suit.<sup>20</sup>

The optimized geometric parameters of the  $S_4$  form are included in Table 4. The HF approximation reproduces the experimental bond lengths to within  $\pm 0.02$  Å, but the calculated P–N–P angle is about  $6^\circ$  larger than the experimental value, resulting in a flatter ring conformation. Consequently, the calculated dihedral angles Φ(PNP) and the o.o.p. coordinates are considerably smaller than the experimental values. On the other hand, the B3LYP method predicts the bond lengths

too long, but reproduces the ring bond angles, dihedral angles, and the o.o.p. coordinates much better than the HF approximation.

### Conclusion

The eight-membered P<sub>4</sub>N<sub>4</sub> heterocycle of the P<sub>4</sub>N<sub>4</sub>F<sub>8</sub> molecule in the crystalline state is not planar, nor chair-shaped as proposed by McGeachin and Tromans and Jagodzinski and Oppermann,<sup>2</sup> respectively, but defines a saddle with the P atoms arranged in a common plane. Above the phase transition, the structural model based on ordered molecules as used in the literature is a superposition of two individual sites related by a center of inversion. The quasiplanar eight-membered P–N skeleton of the averaged molecule above the phase transition, **1a**, represents a projection of the P<sub>4</sub>N<sub>4</sub> saddle of a discrete molecule to the plane defined by the four P atoms. As a consequence, the P–N distances (ca.  $1.52$  Å) as well as the P–N–P angles (ca.  $146.6^\circ$ ) of the averaged molecules deviate systematically from their true values derived with high precision for the ordered molecules below the phase transition, **1d** (ca.  $1.543$  Å and  $140.4^\circ$ ), and by means of a split-atom model with reduced precision for the disordered molecules above the phase transition, **1b** (ca.  $1.55$  Å,  $139.95^\circ$  and  $1.533$  Å,  $143.6^\circ$ ). The unit cells of the two modifications are closely related, with the cell of **1d** derived from the cell of **1a/1b** by doubling the  $c$  axis and removing of one-half of the symmetry elements.

**Acknowledgment.** Dedicated to Professor Dr. Oskar Glemser on the occasion of his 90th birthday. R.H. and H.O. gratefully acknowledge generous financial support by the Fonds der Chemischen Industrie. They also thank the Research Centre Jülich (KFA, Germany) for access to substantial computer time. A.J.E. and J.M.S. thank the National Science Foundation (Grant CHE-9720365) and BNFL plc for financial assistance. Dr. M. Sasaoka, Otsuka Chemical Company, Japan, generously provided the N<sub>4</sub>P<sub>4</sub>Cl<sub>8</sub>. The single-crystal CCD X-ray facility at the University of Idaho was established with the assistance of NSF Idaho EPSCoR and the M. J. Murdock Charitable Trust, Vancouver, WA. A.J.E. is grateful to the Indian Institute of Technology, Kanpur for a sabbatical leave.

**Supporting Information Available:** Tables of experimental data and figures giving DSC scans showing the phase change on cooling and heating N<sub>4</sub>P<sub>4</sub>F<sub>8</sub> and experimental and calculated molecular intensities for short and long nozzle-to-plate distances and residuals (PDF). This material is available free of charge via the Internet at <http://pubs.acs.org>.

JA016015U

(20) Frisch, M. J.; Trucks, G. W.; Schlegel, H. B.; Scuseria, G. E.; Robb, M. A.; Cheeseman, J. R.; Zakrzewski, V. G.; Montgomery, J. A.; Stratman, R. E.; Burant, J. C.; Dapprich, S.; Millam, J. M.; Daniels, A. D.; Kudin, K. N.; Strain, M. C.; Farkas, O.; Tomasi, J.; Barone, V.; Cossi, M.; Cammi, R.; Mennucci, B.; Pomelli, C.; Adamo, C.; Clifford, S.; Ochterski, J.; Petersson, G. A.; Ayala, P. Y.; Cui, Q.; Morokuma, K.; Malick, D. K.; Rabuck, A. D.; Raghavachari, K.; Foresman, J. B.; Cioslowski, J.; Ortiz, J. V.; Stefanov, B. B.; Liu, G.; Liashenko, A.; Piskorz, P.; Komaromi, I.; Gomperts, R.; Martin, R. L.; Fox, D. J.; Keith, T.; Al-Laham, M. A.; Peng, C. Y.; Nanayakkara, A.; Gonzalez, C.; Challacombe, M.; Gill, P. M. W.; Johnson, B.; Chen, W.; Wong, M. W.; Andres, J. L.; Gonzalez, C.; Head-Gordon, M.; Replogle, E. S.; Pople, J. A. GAUSSIAN98, Version A6; Gaussian, Inc.: Pittsburgh, PA, 1998.